SCAFFOLDS WITH TUNABLE PROPERTIES CONSTITUTED BY ELECTROSPUN NANOFIBERS OF POLYGLYCOLIDE AND POLY(ε-CAPROLACTONE)

Ina Keridou[1], Lourdes Franco[1,2], Pau Turon[3], Luis J. del Valle[1,2]

Jordi Puiggalí[1,2*]

[1]Departament d'Enginyeria Química, Universitat Politècnica de Catalunya, Escola d'Enginyeria de Barcelona Est-EEBE, c/Eduard Maristany 10-14, Barcelona 08019, SPAIN
[2]Center for Research in Nano-Engineering, Universitat Politècnica de Catalunya, Campus Sud, Edifici C', c/Pasqual i Vila s/n, Barcelona E-08028, SPAIN
[3]B. Braun Surgical, S.A. Carretera de Terrasa 121, 08191 Rubí (Barcelona), SPAIN

Correspondence to: **J. Puiggalí (E-mail: Jordi.Puiggali@upc.edu)**

ABSTRACT

Electrospun scaffolds constituted by different mixtures of two biodegradable polyesters have been prepared. Specifically, materials with well differentiated properties can be derived from the blending of hydrophilic polyglycolide (PGA) and hydrophobic poly(ε-caprolactone) (PCL), which are also two of the most applied polymers for biomedical uses. Electrospinning conditions have been selected in order to get homogeneous and continuous fibers with diameters in the nano/micrometric range. These conditions were also applied to load the different scaffolds with curcumin (CUR) and polyhexamethylene biguanide (PHMB) as hydrophobic and hydrophilic bactericide compounds, respectively. Physicochemical characterization of both unloaded and loaded scaffolds was performed and involved FTIR and ^{1}H NMR spectroscopies, morphological observations by scanning electron microscopy, study of thermal properties through calorimetry and thermogravimetric analysis and evaluation of surface characteristics through contact angle measurements.

Release behavior of the loaded scaffolds was evaluated in two different media. Results pointed out a well differentiated behavior where the delivery of CUR and even PHMB were highly dependent on the PGA/PCL ratio, the capability of the medium to swell the polymer matrix and the diffusion of the selected solvent into the electrospun fibers. All samples showed a bactericide effect in both hydrophilic cell culture and hydrophobic agar media.

Keywords: Polyglycolide, poly(ε-caprolactone), biodegradable polymers, electrospinning, antibacterial scaffolds, curcumin, polyhexamethylene biguanide, drug delivery.

INTRODUCTION

Polyglycolide (PGA) and poly(ε-caprolactone) (PCL) are currently two of the most employed biodegradable and bioresorbable polymers.[1,2] Tissue engineering, orthopaedic devices and drug delivery systems are representative examples were such polymers are extensively used. PGA has significant issues (e.g. relatively high insolubility, rapid degradation and significant local production of glycolic acid) which limit in some cases its application.[2] Nevertheless, the use of PGA based materials is extensive as bioabsorbable surgical sutures[3] and scaffolds for tissue regeneration.[4-7] PCL is characterized by easy processability, low tensile strength and high elongation at breakage, which confers good elastic properties and suitability for tissue engineering applications. This polymer becomes therefore attractive for the preparation of scaffolds based on electrospun micro/nanofibers.[8-10]

The repeat units of PGA and PCL differ on the number of methylene groups (i.e. one and five, respectively) (Figure 1), a feature that leads to a distinct chain flexibility, surface hydrophobicity and mechanical and thermal properties. For example, the melting points of PCL and PGA are 59-64 ºC and 220-225 ºC, respectively, namely a difference of more than 150 ºC.[11] In this way, materials with tuned properties could hypothetically be obtained by a simple blending of different ratios of PGA and PCL if samples were miscible, which is not the usual case. Nevertheless, simple composition changes can give rise to highly differentiated drug delivery systems as previously observed when two hydrophobic polymers like polylactide and PCL were employed.[12]

Scaffolds based on PGA/PCL mixtures have recently merited attention from different points of views as for example: the evaluation of physical and mechanical properties of electrospun fibers,[13] preparation of scaffolds with aligned fibers for neural applications[14] and in-vitro degradation studies.[15]

Electrospinning is one of the most versatile processes for preparing non-woven nanofibers that could be arranged into porous scaffolds.[16-18] This process uses electrostatic forces (10–100 kV) to stretch drops of a polymer dilute solution from a needle tip to a collector. Nowadays, extensive works concern the fabrication of polymer fibers *via* electrospinning and their use in different biomedical applications (e.g. drug delivery, tissue engineering, and diagnostics).[19-21]

In fact, electrospinning is a fast technique and allows an easy preparation of polymer mixtures if a common solvent is found. Furthermore, domains corresponding to the different polymers should be small due to the nanometric dimensions of the produced fibers and consequently an intimate contact between PGA and PCL molecules may be possible.

Incorporation of drugs into electrospun scaffolds is also an easy process since only minor modifications on the processing parameters are required, being also minimal the repercussion on the final geometry due to the usually low amount of loaded drug that is necessary to get a significant pharmacologic effect. Incorporation of several drugs can provide materials with multifunctional properties.[22] In this work the use of a typical bactericide agent (i.e. PHMB) and an anticancerigen drug (i.e. CUR), which in addition has a bacteriostatic effect, were assayed in order to provide a high added value to the new scaffolds.

PHMB is a mixture of cationic oligomers having an average of 7–13 biguanide groups spaced by flexible hexamethylene segments (Figure 1). The high number of biguanide groups lead to a high effectiveness against microorganisms, although chemical characterization is difficult due to the high dispersion of oligomer sizes.[23] Curcumin (CUR) is a molecule constituted by two phenol groups connected by α,β-unsaturated carbonyl groups (Figure 1). These diketones can form stable enols and are readily

deprotonated to form enolates. Curcumin seems to have beneficial effects on various diseases, including multiple myeloma, pancreatic cancer, myelodysplastic syndromes, colon cancer, psoriasis, and Alzheimer's disease.[24,25] CUR is also a pleiotropic molecule capable of interacting with molecular targets involved in inflammation. It has also been recently evaluated as having a bactericide effect since it can produce a membrane leakage of both Gram-negative and Gram-positive bacteria.[26]

The main goal of the present work is the preparation and characterization of electrospun scaffolds with tuned properties in function of their PGA/PCL ratio. To this end electrospun scaffolds constituted by PGA/PCL ratios of 100/0, 80/20, 65/35, 50/50, 35/65 and 0/100 have been considered, optimizing in each case the processing conditions. Special attention is paid to demonstrate the different release behaviour that can be attained by a simple modification of composition, a less complex alternative than that derived from the use of other processes like coaxial electrospinning.[27]

EXPERIMENTAL SECTION

Materials

Curcumin (CUR), polycaprolactone (M_w: 45,000 g/mol) polyglycolide (PGA) (M_w: 180,000 g/mol) and solvents were purchased from Sigma-Aldrich. Cosmocil® (polyhexamethylene biguanide hydrochloride, PHMB) was kindly provided by B. Braun Surgical, S.A. The microbial culture was prepared with reagents and labware from Scharlab. *Escherichia Coli* and *Staphylococcus aureus* bacteria strains were obtained from the Spanish Collection of Type Culture (CECT, Valencia, Spain).

Preparation of fibers by electrospinning

Electrospun fibers were collected on a target placed at different distances (10–25 cm) from the needle tip (inside diameter 0.84 mm). The voltage was varied between 10 and

30 kV and applied to the target using a high-voltage supply (Gamma High Voltage Research, ES30-5W). Polymer solutions were delivered via a single KDS100 infusion syringe pump (KD Scientific, USA) to control the flow rate (from 1 to 5 mL/h). All electrospinning experiments were carried out at room temperature. Unloaded and drug loaded electrospun fibers were prepared using optimized parameters (i.e. collector distance, voltage and flow rate) and solvent conditions (i.e. polymer and drug concentrations). Samples will be named indicating only the PGA weight percentage (e.g., PGA/PCL-100 and PGA/PCL-35 corresponds to PGA only and a mixture with 35% PGA and 65% PCL, respectively. CUR and PHMB content of the electrospinning solution was 1 *w*/*v*-% and 3 *w*/*v*-%, respectively. For comparative purposes PGA/PCL-50 samples only loaded with CUR (1 *w*/*v*-%) or PHMB (3 *w*/*v*-%) were also prepared. The amount of loaded drugs was determined by absorbance measurements as explained below.

Measurements

Infrared absorption spectra were recorded in the 4000–600 cm^{-1} range with a Fourier Transform FTIR 4100 Jasco spectrometer equipped with a Specac model MKII Golden Gate attenuated total reflection (ATR) cell.

^{1}H NMR spectra were recorded with a Bruker AMX-300 spectrometer operating at 300.1 MHz. Chemical shifts were calibrated using tetramethylsilane as the internal standard and $CDCl_3$ ($\delta(^{1}H)$ = 7.26 ppm) and deuterated DMSO ($\delta(^{1}H)$ = 2.50 ppm) as solvents.

Calorimetric data were obtained by differential scanning calorimetry with a TA Instruments Q100 series with T_{zero} technology and equipped with a refrigerated cooling system (RCS). Experiments were conducted under a flow of dry nitrogen with a sample

weight of approximately 5 mg and at heating and cooling rates of 20 °C min^{-1} and 10 ºC min^{-1}, respectively. Calibration was performed with indium.

Thermal degradation was studied at a heating rate of 10 °C min^{-1} with around 5 mg samples in a Q50 thermogravimetric analyzer (TGA) of TA Instruments and under a flow of dry nitrogen. Test temperatures ranged from 50 to 600 °C.

Contact angles (CA) were measured at room temperature with sessile drops using an OCA-15 plus Contact Angle Microscope (Dataphysics, USA) and SCA20 software. Contact angle values of the right and left sides of distilled water drops were measured and averaged. Measurements were performed 10 s after the drop (5 μL) was deposited on the sample surface. All CA data were an average of six measurements on different surface locations.

Detailed inspection of texture and morphology of electrospun samples was conducted by scanning electron microscopy using a Focused Ion Beam Zeiss Neon 40 instrument (Carl Zeiss, Germany). Carbon coating was accomplished by using a Mitek K950 Sputter Coater fitted with a k150× film thickness monitor. Samples were visualized at an accelerating voltage of 5 kV. The diameter of electrospun fibers was measured with SmartTiff software from Carl Zeiss SMT Ltd.

Release experiments

Controlled release measurements were performed with 1 cm × 1 cm square pieces of the different loaded scaffolds. The thickness was always close to 700 μm. These pieces were incubated at 37 °C in an orbital shaker at 80 rpm in tubes of 10 mL for 1 day. Phosphate-buffered saline (PBS) and a 3:7 *v*/*v* mixture of PBS and ethanol were employed as release media. Drug concentration was evaluated by UV absorbance measurements using a Shimadzu 3600 spectrometer. Calibration curves were obtained by plotting the absorbance measured at 428 and 326 nm versus CUR and PHMB

concentrations, respectively. Samples were withdrawn from the release medium at predetermined time intervals. The volume was kept constant by the addition of fresh medium. All drug release tests were carried out using three replicates and the results obtained were averaged.

Antimicrobial test

E. coli and *S. aureus* bacteria were selected to evaluate the antimicrobial effect of PHMB and CUR loaded electrospun fibers. The bacteria were previously grown aerobically to exponential phase in broth culture (5 g/L beef extract, 5 g/L NaCl, 10 g/L tryptone, pH 7.2).

Growth experiments were performed on a 24-well culture plate. All drug (CUR, PHMB or both) loaded scaffolds (1 cm x 1 cm and thickness close to 700 μm) were placed into the plate as well as an unloaded sample that was used as a control. Then, 2 mL of broth culture containing 10^3 colony forming units (CFU) was added to the samples. Cultures were incubated at 37 °C and agitated at 80 rpm. Aliquots of 100 μL were taken at predetermined time intervals for absorbance measurement at 595 nm in a microplate reader (every 2 h for 8 h, and after 22, 24 and 48 h from the starting time). Thus, turbidity was directly related to the relative bacterial growth by considering the maximum growth attained in the absence of any polymeric matrix (control). Experiments were performed in quadruplicate and the results averaged.

In order to perform a qualitative evaluation, the drug (CUR, PHMB or both) loaded pieces and a commercial gentamicin dose (10 μg), which was used as a control, were placed onto an agar diffusion plate and seeded separately with 10^4 CFU/mL of each bacterium. The culture medium was prepared with 37 g Brain Heart Infusion broth, 10g Bacto™ Agar in 1 L of Milli-Q water and sterilized in an autoclave at 121 ºC for 15 min. Plates were filled with 15 mL of medium and left to rest at room temperature to

allow solidification of the medium. Inhibition halo images were taken after incubation of samples with bacteria at 37 ºC for 24 h.

RESULTS AND DISCUSSION

Electrospinning of PGA/PCL mixtures

PCL is soluble in a wide variety of organic solvents and therefore the preparation of electrospun micro/nanofibers with continuous morphology and uniform distribution has been successfully described for a high variety of solvents (e.g. acetone/chloroform 33% *v*/*v* or ethanol/chloroform 33% *v*/*v* mixtures). On the contrary, PGA is scarcely soluble and consequently electrospinning is practically limited to the use of 1,1,1,3,3,3,-hexafluoroisopropanol (HFIP). Therefore, all experiments were performed employing HFIP in order to have the most similar conditions for all selected blends. Sharifi and collaborators[13] demonstrated that this solvent was appropriate to get scaffolds from PGA/PCL mixtures up to a 50% content of PGA.

Electrospinning parameters were optimized to get fibers with an average diameter close to 1 μm in order to avoid an instantaneous drug release caused by the presence of nanofibers with a very small cross section.

It is well known that fiber diameter is strongly influenced by polymer concentration which was, therefore, kept practically constant and high (i.e. 8 wt-%) for all PGA/PCL blends. Experimental conditions were also optimized for each polymer blend to avoid typical problems like bead formation and to obtain a similar diameter distribution. The selection process was complex since multiple parameters had to be taken under consideration and a clear optimization strategy did not exist. Nevertheless, an iterative study was carried out considering the variation of the voltage for intermediate values of the flow rate and the collector distance. Next steps corresponded to the evaluation of the

effect of the flow rate and finally of the collector distance, readjusting the selected voltage after each study. Note that the study was carried out for the different blends and the selection of parameters was also performed trying to minimize differences between the final electrospun fibers.

The selection of the spinning voltage (*V*) was essential to ensure a stable, conical liquid jet which minimized bead formation and guaranteed again a diameter over a minimum value. Flow rate was also important to get sufficiently high diameters while complete solvent evaporation was assured. These requirements are favoured at high and low rates, respectively. The distance between the collector and the syringe tip (*h*) was varied in order to get the minimum value and avoid typical problems of coalescence derived from a non-completed solvent evaporation. Note that the surface tension and the solution viscosity, which usually have a strong influence on fiber morphology, could not be modified since the solvent and polymer concentration were not changed.

All selected PGA/PCL mixtures could finally be electrospun using the same parameters as summarized in Table 1. The deduced parameters were slightly different from those reported in the previous work of Aghdam et al.[13] (i.e. 17 kV, 10 cm and 2 mL/h for voltage, distance and flow rate, respectively) since we were interested to get fibers with greater diameters as previously indicated. Comparatively, we clearly increased the flow rate as well as the polymer concentration in the electrospun solution (i.e. from 2 to 3 mL/h and from 6% to 8%, respectively). The PCL homopolymer sample required special conditions due to its clearly lower molecular weight (M_w: 45,000 g/mol). Note for example that a concentration of 6% was necessary for the electrospinning of high molecular weight (M_w: 80,000 g/mol) PCL samples[13]. Therefore, polymer concentration was increased from 8 wt-% to 18 wt-% to get a solution with a

sufficiently high viscosity. At the same time, applied voltage was decreased from 20 kV to 15 kV and the collector distance was increased from 10 cm to 19 cm.

Scanning electron micrographs of the electrospun samples (Figure 2) demonstrated that continuous and straight fibers with a smooth surface could be obtained in all cases. Representative histograms of the diameter distributions for the different electrospun samples are given in Figure 3. Morphology of PGA/PCL-0 (i.e. the PCL homopolymer) electrospun fibers was clearly different since the average diameter remained in the nanoscale (155 nm) despite the great changes on the electrospun parameters that were applied in order to increase the diameter. In fact, the changes were only successful in producing continuous and homogeneous fibers, but had not a significant effect on the final diameter size. Micrographs of scaffolds obtained from the selected PGA/PCL blends showed also the presence of a small proportion of thin fibers (i.e. less than 10% for PGA/PCL-35). This could be attributed to PCL rich fibers, being less abundant as the PGA composition in the electrospun solution increased. Note for example the differences between the PGA/PCL-35 and PGA/PCL-80 samples (Figure 3). The presence of the small population of thin fibers may suggest the occurrence of a minor phase separation during the electrospinning process (e.g. just before ejection from the drop). The PGA/PCL-20 sample was discarded form further studies since nanofibers were highly predominant and consequently the derived scaffolds were not useful for establishing a simple study on the drug release and composition dependence (i.e. without a significant influence of the fiber diameter). Histograms corresponding to the high diameter population showed always a Gaussian distribution with an average diameter that progressively increased (i.e. from 750 to 1500 nm) as the PGA content in the electrospun solution did. This feature is significant since it suggests that PCL is also incorporated in the coarse fibers.

Basic characterization of PGA/PCL-x scaffolds

FTIR spectra of the electrospun samples showed logically the characteristic bands of each homopolymer as displayed in Figure 4 for the representative PGA/PCL-50 sample. This point is clearly observed through the presence of carbonyl bands at 1746 cm^{-1} and 1721 cm^{-1} that corresponds to PGA and PCL, respectively. Note that the intensity of these bands changed according to the final composition. The 1500-1300 cm^{-1} region is also significant since the multiple peaks observed for PCL became progressively simplified in such a way that only two peaks corresponding to crystalline PGA (at 1415 cm^{-1}) and amorphous PGA (at 1395 cm^{-1}) could be detected when the PCL content decreased. Similar conclusions could be obtained from the disappearance of PCL bands at 1237 cm^{-1} and 961 cm^{-1} or the appearance of PGA bands at 1081 cm^{-1} when the PGA content increased. The analysis of the C-O region (at ca. 1145 cm^{-1}) was more complex due to the overlapping of characteristic bands of both polymers.

Composition of prepared scaffolds was determined from ^{1}H NMR spectra where signals corresponding to glycolic acid (4.95 ppm) and ε-caprolactone (4.17, 2.45, 1.74-1.67 and 1.44-1.42 ppm) units appeared well differentiated (Figure 5). The glycolic acid content (GA wt-%) was evaluated through the areas of signals observed at 4.95 and 4.17 ppm, which correspond to $O(CH_2)$ protons of glycolyl and ε-caproyl units, respectively:

$$GA\ w\text{-}t\% = [A_{4.95} \times 58 / (A_{4.95} \times 58 + A_{4.17} \times 114)] \times 100 \qquad (1)$$

where 58 and 114 correspond to the molecular weight of glycolyl and ε-caproyl units, respectively.

Logically, global composition of the scaffold should agree with the feed polymer ratio in the electrospun solution, but it is not clear that a homogeneous and regular fiber deposition was achieved. Therefore, analysis was performed by sampling each electrospun scaffold and taking data from five points regularly spaced along the

diagonal of 5 cm × 5 cm square piece. Thus, GA wt-% of 80 ± 2, 66 ± 3, 50 ± 4 and 34 ± 3 were determined for PGA/PCL-80, PGA/PCL-65, PGA/PCL-50, PGA/PCL-35 samples, respectively.

Figure 6 shows the typical protocol performed for the calorimetric study of the different scaffolds. This consists of a first heating scan of the electrospun sample in order to detect crystallinity of the processed sample, a cooling scan to determine the crystallization behavior after erasing thermal history by keeping the sample 10 ºC above fusion, a second heating scan to determine the behavior of the melt crystallized sample, and finally a third heating scan of a sample quenched from the melt at the maximum cooling rate allowed by the equipment (50 ºC min^{-1}).

Specifically, traces for PGA/PCL-50, as representative scaffold due to its intermediate composition, are shown in Figure 6. The corresponding data for all studied samples are summarized in Tables 1 and 2. Well differentiated melting and crystallization peaks that can be associated to each homopolymer can be detected for the PGA/PCL-50 sample at 55.7 ºC and 221.4 ºC (for fusion) and 29.3 and 185.7 ºC (for crystallization). Melting temperatures are in full agreement with those reported[11] (59-64 ºC and 220-225 ºC) for the two homopolymers, indicating that well differentiated crystalline phases were developed, even for the electrospun processed sample. For other compositions, the behavior was similar with logical variations of peak temperatures that move in a wider range (e.g. 40 ºC- 57 ºC and 12 ºC- 31 ºC for the fusion and crystallization of PCL, respectively). The DSC heating trace of the PGA/PCL-50 electrospun sample (Figure 6 and Table 2) shows two significant features concerning PCL and PGA domains that deserve attention:

a) PCL is crystallized easily during electrospinning probably as a consequence of the high orientation achieved, especially for the narrow fibers enriched on PCL. Two

melting peaks were detected (Figure 6a, Table 2) suggesting the existence of two lamellar populations, with the narrower ones being sufficiently stable to prevent its reordering process during heating. The degree of crystallinity was close to 38% taking into account a PCL content of 50 wt-% and the reported enthalpy for a 100% crystalline sample (136 J/g).[28] Note that a single peak (55 ºC) corresponding to reordered lamella having a lower crystallinity (i.e. close to 26%) was observed for melt crystallized (Figure 6c) and quenched (Figure 6d) samples. Therefore, crystallization of PCL was in such cases hindered for the previously formed PGA crystalline domains, which is not the case of samples prepared by electrospinning. In fact the crystallization peak of PCL was very low during the cooling scan from the melt state (Figure 6b), being this feature a clear demonstration that when the PCL remains at the lowest temperature is crystallized slowly before performing the subsequent heating scan. A similar behavior can be deduced from the melt quenched sample, justifying the similar crystallinity that was achieved.

b) The electrospinning process has also allowed the crystallization of PGA, but the degree of crystallinity (39% when the reported value of 139 J/g for a 100% crystalline sample[29] was considered, as well as a PGA content of 50 wt-% and the enthalpy of exothermic peaks subtracted) was clearly lower than the obtained one from melt crystallized or melt quenched samples. Both were close to 68% since PGA was able to crystallize under the maximum cooling rate allowed by the equipment. Note also that the electrospun sample showed a clear cold exothermic crystallization peak at 69.8 ºC and even a very small hot crystallization peak at 215 ºC. The melting enthalpy and the final crystallinity (achieved during the heating process) became similar to those determined for the melt crystallized samples. A single melting peak close to 221 ºC was observed for the electrospun sample, being indicative of a lamellar reorganization

during heating. Note that a double melting peak was only detected for the melt crystallized sample at the slow rate of 10 ºC min^{-1} since in this case thinner and stable lamellae were formed and a peak at 214 ºC corresponding to the non-reordered crystals could be detected.

Calorimetric data of the different electrospun samples are compared in Table 3, making it clear that melting enthalpies of PCL and PGA domains logically decreased and increased, respectively with the PGA content. More interestingly, the PGA cold crystallization peak for fibers with a PGA content lower than 80% was enhanced when the PCL content increased, indicating a greater difficulty to get crystalline PGA domains during electrospinning. It is clear that PCL was well-mixed inside the fibers and hindered PGA crystallization during the electrospinning process. Note also that the cold crystallization temperature increased for higher PCL contents demonstrating again the greater difficulty of PGA to crystallize from the mixed phase. A contrary effect was observed for the PGA cold crystallization peak of samples with a high PGA content (i.e. $\geq$ 80 wt-%) since in this case electrospinning was able to render highly ordered PGA domains.

Final crystallinity of PCL domains was relatively high (26-62%) for all samples as well as that of PGA domains after thermal treatment of samples (i.e. 37-57%) (cold and hot crystallization processes). These values were also in agreement with those determined from melt crystallized samples (Table 3). Nevertheless, the crystallinity of PGA domains of electrospun samples before thermal recrystallization processes showed moderate values (i.e. 26-33%) and a regular increase with the PGA content.

Thermogravimetric analysis (Figure 7) shows that the behavior of the electrospun blends is not exactly defined by a simple combination of TGA curves of the corresponding homopolymers. Note that the degradation of PCL is characterized by a

single DTGA peak at 408 ºC (for a heating rate of 10 ºC min^{-1}) without char yield, while degradation of PGA is complex with a predominant peak at 388 ºC, a shoulder at a lower temperature (345 ºC) and a significant char yield (1.7 wt-%). DTGA curves of blends, as shown for the representative PGA/PCL-50 sample, were also complex and revealed two main peaks with a variable intensity depending on composition. The first one appeared at an intermediate position to those detected for the two decomposition steps of PGA (i.e. 362 ºC), while the second one appeared at a significantly lower temperature (388 ºC) than the one found for PCL. This observation clearly indicates that the degradation of the PCL component was accelerated by the decomposition products of the most unstable PGA component. Note that PGA/PCL-50 was practically degraded (remaining weight of 12%) before achieving the temperature of the DTGA peak of PCL. Nevertheless, degradation gave rise to a significant char yield, even higher than the one determined for the PGA homopolymer.

X-ray diffraction patterns of the electrospun samples showed the characteristic reflections of both homopolymers. Thus, three Bragg peaks at 0.416, 0.403 and 0.373 nm, which correspond to the (110), (111) and (200) reflections of the orthorhombic unit cell (a = 0.747 nm, b = 0.498 nm, c (fiber axis) = 1.705 nm) of poly(ε-caprolactone),[30,31] were determined for the PGA/PCL-0 sample (Figure 8a). PGA/PCL-100 showed two main peaks at 0.399 and 0.309 nm that correspond to the (110) and (020) reflections of the orthorhombic unit cell of polyglycolide (Figure 8c) (a = 0.522 nm, b = 0.619 nm, c (fiber axis) = 0.702 nm).[32] In addition, a clear amorphous halo centered around 0.455-0.446 nm was always observed, making it possible to determine the degree of crystallinity of all samples by the deconvolution of the WAXD patterns. Results pointed out that PCL is crystallized more easily than PGA during electrospinning (i.e. degree of crystallinities of 86% and 49% for PCL and PGA,

respectively), a feature that could be related with the higher molecular orientation that could be attained when the diameter of the electrospun fibers decreased. Diffraction profiles of the different blends showed always a global crystallinity higher than the determined one for the PGA sample. Results demonstrated the capability of PCL to crystallize, even in the presence of PGA, and pointed out a clear phase separation of the two copolymers during the electrospinning process. Deconvolution confirmed the DSC results which indicated that final crystallinity can be attributed mainly to the PCL phase. Thus, the representative PGA/PCL-50 had a final crystallinity of 68%, with 47% and 21% being the values deduced for PCL and PGA domains respectively.

The increase of the PGA content in the electrospun scaffolds lead logically to an increase of the hydrophilicity of the samples as revealed by contact angle measurements (Figure 9). Scaffolds of the PCL homopolymer were highly hydrophobic, with the contact angle being close to 130º. The hydrophobic surface was kept up to a PGA content of 65 wt-%, but a monotonous decrease of the contact angle was detected as the PGA content increased (i.e. from 130º to 114º). Note that the influence of the PGA content could be slightly counterbalanced by the increase of the surface roughness. Specifically, the increase of the fiber diameter size should lead to a more hydrophobic surface according to the Wenzel equation.[33] The importance of the surface effect is evident when data reported for scaffolds made up of fibers with smaller diameters[13] are considered (e.g. the contact angle of PCL decreased from 130 º to 118º when diameters decreased from 155 nm to 86 nm). The scaffold with a PGA content of 80 wt-% became completely hydrophilic, with the contact angle being similar to that determined from the corresponding homopolymers (i.e. < 5º). In summary, physical properties (e.g. hydrophobic/hydrophilic surface characteristics) of the new scaffolds could be tuned by

changing the polymer composition, making it possible to have a fine control at high/moderate PCL content (i.e. ≥ 35 wt-%).

CUR and PHMB loaded PGA/PCL-*x* electrospun scaffolds

Electrospinning parameters could be maintained when both CUR and PHMB compounds were incorporated in the HFIP solution of the corresponding polymer mixture. Continuous fibers were always obtained and in general a small decrease of the fiber diameters (Table 1) with respect to those determined for the unloaded samples was detected. Probably the most important effect was the increase of the conductivity of the electrospinning solutions as a consequence of the presence of the cationic PHMB compound. In any case, the reduction of diameter was scarce and lower than 30%. An increase of the diameter was only detected for the PGA/PCL-0 homopolymer, but it should be pointed out that in this case the concentration of the polymer was well differentiated from all the other samples. Incorporation of PHMB had a higher effect on the reduction of diameter as could be deduced from the values of 749, 537, 587 and 636 nm determined for the PGA/PCL-50 unloaded sample and that loaded with PHMB+CUR, PHMB and CUR, respectively. Figure 10 shows that the texture of the fibers was always smooth and that the presence of crystals corresponding to each loaded compound could not be detected. The appearance of fibers clearly changed after exposure to an aqueous release medium (i.e. PBS/ethanol mixture) since the presence of pores and longitudinal striations were evident (Figure 11). This feature could be related to an initial swelling, the delivery of soluble compounds and a final shrinkage after drying. In fact, the diameter size decreased after exposure to the indicated medium by approximately 10-15% (e.g. the diameter of PGA/PCL-50 loaded with PHMB+CUR decreased from 537 to 475 nm).

The presence of domains associated to CUR or PHMB crystals could be discarded considering both X-ray diffraction patterns and DSC heating scans (not shown) since characteristic reflections or melting peaks were not detected. Thus, the crystallization of the drugs during the electrospinning process seems to be prevented in agreement with the absence of crystals deduced from morphological observations. This feature is important since activity of the added compounds should be higher in the amorphous state. On the other hand, the influence of the drugs on calorimetric parameters (e.g. crystallization and melting temperatures and the corresponding enthalpies) were not highly significant as expected when drugs were not incorporated into the crystalline domains of PGA and PCL.

Incorporation of CUR and PHMB had a strong influence on the thermal stability of the prepared scaffolds as shown in Figure 12 for the PGA/PCL-50 representative sample. The most important feature is a clear thermal destabilization, with the onset degradation temperature being decreased by at least 40 ºC. The DTGA profiles changed also remarkably and a great decrease on the degradation peak temperature associated to the first decomposition step was observed. Thus, values of 262-263 ºC and 303 ºC were determined for the samples loaded with CUR and PHMB, respectively, in contrast with the temperature of 362 ºC detected for the unloaded sample. The weight loss associated to this step was close to 35% for both loaded samples, a value that was clearly higher than the amount of incorporated drug and this points out an accelerated degradation of the most unstable PGA homopolymer. In fact, the degradation process may be logically enhanced by the decomposition products of CUR and PHMB, which were reported to appear at lower temperatures than the onset of PGA decomposition. Specifically, the most negative effect was observed for PHMB, in which degradation was reported to start at 230 ºC,[34] although the more significant decomposition steps occur at 364 ºC

and 473 ºC.[35] The degradation of CUR is characterized by two steps that corresponded to single processes with degradation peaks at 292 ºC (mass loss of 33.8%) and 486 ºC (mass loss of 66.2%).[36]

DTGA profiles of loaded electrospun PGA/PCL samples showed also a second and predominant degradation peak at temperatures close to that observed in the unloaded samples. This peak appears at a slightly higher temperature (i.e. 407 ºC with respect to 401 ºC) for the CUR loaded sample or at a lower temperature when PHMB was incorporated (e.g. see the complex peak near 390 ºC). In addition, these samples showed an additional decomposition step at 450 ºC that could be linked with the observed one for PHMB.[35] Degradation was also characterized by an increase of the char yield (i.e. from 2% to 6%, 10% or 14% when CUR, PHMB or both compounds were respectively incorporated).

CUR and PHMB release from PGA/PCL-*x* electrospun scaffolds

PGA/PCL electrospun scaffolds showed a well differentiated release behavior in function of their composition, the hydrophilicity of the drug and the selected release medium. However, in all cases, the release occurred according to two different steps: a fast delivery of molecules that were probably located near or on the high surface area of micro/nanofibers, and a subsequent slow delivery that should involve the diffusion of molecules through the polymer matrix to the release medium. In fact, this process is usually described by a two-step kinetic model that follows Higuchi[37] and first-order[38] (2) equations for 0-60% and 40-100% of the release, respectively.[39]

Time evolution of CUR release percentages during exposition to an aqueous PBS medium is displayed in Figure 13a for all studied compositions. Plots revealed a typical initial fast release that covers a period of 100 min and a subsequent slow release that reaches a saturation level and hence achievement of equilibrium. Saturation level

diminished significantly by increasing the PCL ratio (i.e. from 65% to 5%), demonstrating the capability to tune the release behavior by a simple modification of the ratio between two of the most employed biodegradable polyesters. Logically the hydrophobic CUR had a higher affinity with the polymer matrix when it was enriched on the more hydrophobic PCL component. A relatively good linear dependence was found between the CUR saturation level (y) and the PGA wt-% (x) (i.e. $y = 0.56\,x + 12$, $r = 0.98$). The slopes of the release curves at the beginning also indicated an increase of the release rate with the PGA content.

Addition of ethanol to the release medium facilitated the delivery of both CUR and PHMB since this solvent enhanced the swelling of fibers and also increased the solubility of both compounds. This effect is illustrated in Figure 13b where the differences between the saturation levels were minimized (i.e. release percentages varied between 98 and 92% after an exposure of 650 min). Nevertheless, the above indicated trend concerning the release rate was clear at short exposure times. Thus, release percentages decreased from 75% to 55% after 25 min of exposure when the PGA wt-% decreased. Presence of PHMB enhanced also the delivery of CUR as illustrated in Figure 13b for PGA/PCL-50 loaded only with CUR (see the dashed line). Note that in this case, the saturation level decreased up to 60%, although it remains higher than observed for the PBS medium. This point gives a second argument to explain differences on the release and emphasizes the importance of increasing the hydrophilicity of the fiber (as expected by the incorporation of PHMB) to favour the release in an aqueous media as will be discussed below for PHMB.

The release of PHMB in PBS (Figure 13c) also showed the achievement of a saturation level, which was clearly higher than the one observed for CUR (i.e. see dashed lines for a direct comparison). This feature can be well justified considering the higher solubility

of PHMB in the aqueous medium due to its higher hydrophilic character and the lower capability of the polymer matrix to retain the bactericide component. In general, the observed trend is that the saturation level increased with the PGA content, which is in contradiction with a higher affinity of the drug with the matrix. Note that the release should be higher by increasing the hydrophobic PCL ratio. Therefore, in this case, results strongly support the hypothesis that the delivery mainly depends on the ability of the solvent to penetrate inside the fiber, which is logically higher when the PGA content increases, but must also depend on other factors such as crystallinity and diameter size.

Thus, a bad linear dependence was found between the PHMB saturation level (y) and the PGA wt-% (x) (i.e. $y = 0.29\ x + 62.8$, $r = 0.77$).The regression coefficient increased to 0.94 when the release of the more amorphous PGA/PCL-50 sample was not considered ($y = 0.31\ x + 58.9$), a feature that supports the different diffusion of solvent inside the polymeric matrices.

Antibacterial activity of PGA/PCL-*x* electrospun scaffolds

The antimicrobial effect of PHMB and CUR loaded matrices was evaluated quantitatively by considering the growth curves of Gram-negative (*E. coli*) and Gram-positive (*S. aureus*) bacteria, (Figures 14a and 14b, respectively). The unloaded matrix was highly susceptible to bacterial infection and biofilm formation, with a latency phase that extended over a period of 6 h and that was followed by an exponential growth (log) phase. Bacterial growth was completely inhibited for all samples loaded with PHMB. The only remarkable difference was the higher time required for the PGA/PCL-0 sample to attain a 0% relative growth of the less susceptible *E. coli* bacterium (Figure 14a). This result seems coherent considering the lower observed release of both loaded drugs from this more hydrophobic composition. A total inhibition was not attained

when samples were only loaded with CUR, for example the detected decrease of bacterial growth was close to 35% and 73% for *E. coli* and *S. aureus*, respectively, for the PGA/PCL-50 sample. In fact, CUR has a lower bactericide effect than PHMB and furthermore its release was also lower as explained before. The bactericidal effect was qualitatively corroborated by agar tests, i.e. measuring the inhibition halos around scaffold pieces (Figure 15). This method may be problematic to evaluate the bactericidal effect caused by hydrophilic drugs such as PHMB since their release in the hydrophobic agar medium may be difficult. Results (Figure 15) point out that inhibition halos were significant for all loaded samples, regardless of the type of bacteria, and even when only CUR was loaded. Note that no inhibition halo was observed for the unloaded PGA/PCL-50 sample, which can be considered as the negative control.

CONCLUSIONS

Electrospinning of HFIP solutions of PGA and PCL homopolymer mixtures becomes a simple method to obtain materials with tuned properties in terms of hydrophilic/hydrophobic character and drug delivery behavior. Furthermore, the system is interesting since it involves two of the most applied biodegradable polyesters in the biomedical field. Electrospinning parameters can be well suited to get, homogeneous and continuous fibers in the nano/micrometer diameter range, even when pharmacologically active compounds (i.e. CUR and PHMB) were loaded. Crystallinity and in general thermal properties of new scaffolds were dependent on the PGA/PCL ratio, where the samples with an intermediate composition were logically more amorphous. The selected CUR and PHMB compounds could be effectively loaded into electrospun fibers, while their crystallization was possible to be avoided. Incorporation

of CUR and PHMB had a remarkable effect on the thermal stability of the loaded scaffolds, with the addition of the cationic PHMB being more problematic.

A well-differentiated CUR release in PBS medium was observed depending on the PGA/PCL ratio. In all cases, the release achieved a saturation level that decreased with the increase of the content of the hydrophobic PCL component. Release of PHMB was also dependent on the composition and more specifically increased when diffusion of the medium into the polymer matrix was favoured by the increase of sample hydrophilicity and the decrease of crystallinity. In the same way the release of CUR was enhanced when scaffolds were also loaded with the hydrophilic PHMB.

All scaffolds loaded with CUR and PHMB showed a bactericide effect independently of employing a hydrophilic or a hydrophobic culture medium. Nevertheless, CUR loaded samples had a clearly lower activity than PHMB loaded ones.

Acknowledgements. Authors are in debt to supports from MINECO and FEDER (MAT2015-69547-R). The work has also been carried out under a research agreement between B. Braun Surgical, S. A. and the Universitat Politècnica de Catalunya. Ms I. Keridou thanks financial support from B. BRAUN Surgical S.A.

REFERENCES

1. M. Martina, D.W. Hutmacher, *Polym. Int.* **2007**, *5*6, 2.

2. B. D. Ulery, L. S. Nair, C. T. Laurencin, *J. Polym. Sci. B Polym. Phys.* **2011**, *49*, 12.

3. C. C. Chu, , A. J. von Fraunhofer, H. P. Greisler, *Wound Closure Biomaterials and Devices*, CRC Press, Florida, **1997**.

4. S. Knight, C. Erggelet, M. Endres, M. Sittinger, C. Kaps, E. Stussi, *J. Biomed. Mater. Res. Part B: Appl. Biomater.* **2007**, *83*, 2.

5. N. Dunne, V. Jack, R. O'Hara, D. Farrar, F. Buchanan, *J. Mater. Sci. Mater. Med.* **2010**, *21*, 8.

6. N. Mahmoudifar, P. M. Doran, *Biomater.* **2010**, *31*, 14.

7. C. Erggelet, K. Neumann, M. Endres, K. Haberstroh, M. Sittinger, C. Kaps, *Biomater.* **2007**, *28*, 36.

8. W. J. Li, J.A. Cooper, R.L. Mauck, R. S. Tuan, *Acta Biomater.* **2006**, *2*, 4.

9. A. Luciani, V. Coccoli, S. Orsi, L. Ambrosio, P.A. Netti, *Biomater.* **2008**, *29*, 36.

10. S. Chung, N. P Ingle, G. A. Montero, S. H Kim, M. W. King, *Acta Biomater.* **2010**, *6*, 6.

11. D. K Platt, *Biodegradable polymers market report*. Smithers Rapra Publishing, Salesbury, United Kingdom, **2006**.

12. L. J. del Valle, R. Camps, A. Díaz, L. Franco, A. Rodríguez-Galán, J. Puiggalí, *J. Polym. Res.* **2011**, *18*, 6.

13. R. M. Aghdam, S. Najarian, S. Shahesi, S. Khanlari, K. Shaabani, S. Sharifi, *J. Appl. Polym. Sci.* **2012**, *124*, 123.

14. F. A. Paskiabi, E. Mirzaei, A. Amani, M.A. Shokrgozar, R. Faridi-Majidi, *Int. J. Biol. Macromol.* **2015**, *81*, 1089.

15. J.B. Jonnalagadda, I.V. Rivero, J. Warzywoda, *J. Biomater. Appl.* **2015**, *30*, 472.

16. D. H. Reneker, I. Chun, *Nanotechnology* **1996**, ***7***, 3.

17. D. Li, Y. Xia. *Adv. Mater.* **2004**, *16*, 14.

18. J. M. Deitzel, J. Kleinmeyer, D. Harris, N.C. Beck Tan, *Polymer* **2001**, *42*, 1.

19. G. Yang, X. Li, Y. He, J. Ma. G. Ni, S. Zhou, *Prog. Polym. Sci.* in press **2018**, https://doi.org/10.1016/j.progpolymsci.2017.12.003.

20. L. Li, G. Zhou, Y. Wang, G. Yang, S. Ding, S. Zhou, *Biomater.* **2015**, *37*, 218.

21. G. Yang, J. Wang, Y. Wang, L. Li, X. Guo, S. Zhou. Acs Nano **2015**, *9*, 1161.

22. E. Llorens, L. J. del Valle, J. Puiggalí, *J. Appl. Polym. Sci.* **2016**, *133*, 8.

23. K. Kaehn, *Skin Pharm. Phys*. **2010**, *23*.

24. H. Hatcher, R. Planalp, J. Cho, F.M. Torti, S.V. Torti, *Cell. Mol. Life Sci.* **2008**, *65*, 11.

25. Y. Jiao, J. Wilkinson, X. Di, W. Wang, H. Hatcher, N.D. Kock, R. D'Agostino, M. A. Knovich, F.M. Torti, S.V. Torti, *Blood*, **2009**, *113*, 2.

26. P. Tyagi, M. Singh, H. Kumari, A. Kumari, K. Mukhopadhyay, *PLoS One* **2015**, *10*, 3.

27. E. Llorens, H. Ibañez, L. J. del Valle, J. Puiggalí, *Mater. Sci. Eng. C.* **2015**, *49*.

28. V. Grescenzi, G. Manzini, G. Calzolari, C. Borri, *Eur. Polym. J.* **1972**, *8*, 3.

29. D. Cohn, H. Younes, G. Marom, *Polymer* **1987**, *28*, 12.

30. Y. Chatani, T. Okita, H. Tadokoro, Y. Yamashita, **1970**, *1*, 5.

31. T. Iwata, *Polym. Int.* **2002**, *51*, 10.

32. Y. Chatani, K. Suehiro, Y. Okita, H. Tadokoro, K. Chujo, *Macromol. Chem.* **1968**, *113*, 1.

33. R. Wenzel, *Ind. Eng. Chem*. **1936**, *28*, 8.

34. G. C. East, J. E. Mclntyre. J. Shao, *Polymer* **1997**, *38*, 15.

35. G. de Paula, G. I. Netto, L. H. C. Mattoso, *Polymers* **2011**, *3*, 2.

36. Z. Chen, Y. Xia, S. Liao, Y. Huang, Y. Li, Y. He, Z. Tong, B. Li, *Fodd Chem*. **2014**, *155*.

37. T. Higuchi, *J. Pharm. Sci*. **1963**, *52*.

38. J. G. Wagner, *J. Pharm. Sci*. **1969**, 58.

39. R. Baker, *Controlled release of biologically active agents*. Wiley, New York, **1987**.

FIGURE CAPTIONS

Figure 1. Chemical structures of polyglycolide (PGA), poly(ε-caprolactone), curcumin (CUR) and polyhexamethylene biguanide (PHMB).

Figure 2. SEM micrographs of PGA/PCL-x electrospun fibers prepared under the optimized conditions.

Figure 3. Frequency distribution of the fiber diameter and Gaussian functions of PGA/PCL-x fibers prepared under the optimized conditions.

Figure 4. FTIR spectra (2000-900 cm^{-1}) of PGA/PCL-*x* electrospun fibers.

Figure 5. ^{1}H NMR spectrum of the representative PGA/PCL-35 electrospun sample. The selected spectrum correspond to the sampling spot with the farthest composition from the theoretical one.

Figure 6. DSC traces showing the typical protocol followed for the PGA/PCL-50 electrospun sample: a) Heating scan of the initial sample, b) Cooling scan from the melt state, c) Heating scan of the melt crystallized sample and d) Heating scan of a melt quenched sample.

Figure 7. TGA (solid lines) and DTGA (dashed lines) curves of PGA-PCL-100 (blue), PGA/PCL-50 (green) and PGA/PCL-0 (red) electrospun scaffolds.

Figure 8. X ray diffraction profiles with the corresponding deconvolution of PGA/PCL-0 (red), PGA/PCL-50 (blue) and PGA/PCL-100 (green) electrospun samples.

Figure 9. Contact angle measurements of PGA/PCL-*x* electrospun scaffolds in distilled water.

Figure 10. SEM micrographs of drug loaded PGA/PCL-50 electrospun scaffolds and frequency distribution of the corresponding fiber diameters.

Figure 11. SEM micrograph of a dried PGA/PCL-50 electrospun scaffold loaded with CUR and PHMB after exposure for 1 day to a PBS/ethanol medium.

Figure 12. TGA (solid lines) and DTGA (dashed lines) curves of unloaded and drug loaded PGA/PCL-50 electrospun scaffolds.

Figure 13. Cumulative CUR (a,b) and PHMB (c) release profiles of the indicated electrospun samples in a PBS (a,c) and PBS/ethanol (7:3 *v*/*v*) medium (b). For comparison purposes cumulative CUR release profiles in a PBS medium are also plotted in (c).

Figure 14. Growth curves of *E. coli* (a) and *S. aureus* (b) in the indicated drug loaded electrospun scaffolds and the unloaded one used as a control.

Figure 15. Images showing inhibition halos on agar plates seeded with *E. coli* (a) and *S. aureus* (b) that were caused by: 1. Gentamicin control, 2. PGA/PCL-50, 3. PGA/PCL-50 +PHMB, 4. PGA/PCL-50 + CUR, 5. PGA/PCL-50 +CUR+PHMB, 6. PGA/PCL-0 + CUR + PHMB, 7. PGA/PCL-35 + CUR + PHMB, 8. PGA/PCL-65 +CUR + PHMB, 9. PGA/PCL-80 + CUR + PHMB and 10. PGA/PCL-100 + CUR + PHMB samples.

Table 1. Selected electrospinning parameters for the preparation of the scaffolds derived from different PGA/PCL mixtures.

Sample	Voltage (kV)	Flow (mL/h)	Distance (cm)	Diameter[a] (nm)	Diameter[b] (nm)
PGA/PCL-0	15	3	19	155 ± 1	306 ± 7
PGA/PCL-35	20	3	10	749 ± 26	536 ± 17
PGA/PCL-50	20	3	10	784 ± 23	567 ± 30
PGA/PCL-65	20	3	10	904 ± 42	740 ± 19
PGA/PCL-80	20	3	10	1190 ± 30	852 ± 19
PGA/PCL-100	20	3	10	1532 ± 33	1267 ± 39

[a]Unloaded samples.
[b]Samples loaded with both PHMB and CUR.

Table 2. Calorimetric data derived from the first heating scan of PCL/PGA-*x* electrospun samples.[a]

Sample	$T_{m,1}$ (°C)	$\Delta H_{m,1}$ (Jg^{-1})	χ_{PCL} (%)	T_{cc} (°C)	ΔH_{cc} (Jg^{-1})	T_{hc} (°C)	ΔH_{hc} (Jg^{-1})	$T_{m,2}$ (°C)	$\Delta H_{m,2}$ (Jg^{-1})	χ_{PGA}[b] (%)	χ_{PGA}[c] (%)
PGA/PCL-0	57.5	84.8	62	-	-	-	-	-	-	-	-
PGA/PCL-35	40.1, 56.9	42.6	48	67.5	3.6	182.5	1.7	220.4	18.2	37	26
PGA/PCL-50	43.2, 55.7	26.3	38	69.8	15.5	182.4	4.3	221.4	38.7	55	27
PGA/PCL-65	39.1, 49.2	12.5	26	62.2	17.5	179.2	8.3	219.5	52.0	57	29
PGA/PCL-80	40.4, 48.9	7.1	26	60.0	13.0	178.4	10.5	220.3	57.5	51	30
PGA/PCL-100	-	-	-	57.3	1.5	128.0	16.1	220.0	67.8	49	33

[a]Subscripts 1 and 2 refer to PCL and PGA, respectively. T_{cc} and ΔH_{cc} indicate the temperature and enthalpy of the cold crystallization peak. T_{hc} and ΔH_{hc} indicate the temperature and enthalpy of the hot crystallization peak.

[b]Crystallinity of the PGA phase determined from the melting enthalpy and the PGA content.

[b]Crystallinity of the PGA phase determined from the melting enthalpy, the PGA content and the substraction of cold and hot crystallization enthalpies.

Table 3. Calorimetric data from the first cooling scan and second heating scan of PGA/PCL-*x* electrospun samples.[a]

Sample	$T_{c,1}$ (°C)	$\Delta H_{c,1}$ (Jg^{-1})	$T_{c,2}$ (°C)	$\Delta H_{c,2}$ (Jg^{-1})	$T_{m,1}$ (°C)	$\Delta H_{m,1}$ (Jg^{-1})	$T_{m,2}$ (°C)	$\Delta H_{m,2}$ (Jg^{-1})
PGA/PCL-0	31.5	65.9	-	-	56.1	69.6	-	-
PGA/PCL-35	30.2	40.0	187.5	25.7	55.4	44.8	211.3, 220.1	24.4
PGA/PCL-50	29.3	18.6	185.7	48.1	55.2	19.7	214.0, 220.9	50.4
PGA/PCL-65	13.3	12.7	185.9	53.5	53.3	13.1	211.0, 220.6	51.5
PGA/PCL-80	12.0	8.6	185.6	59.3	53.2	9.1	210.3, 220.6	53.5
PGA/PCL-100	-	-	187.0	68.1	-	-	212.0, 220.4	67.1

[a]Subscripts 1 and 2 refer to PCL and PGA , respectively.

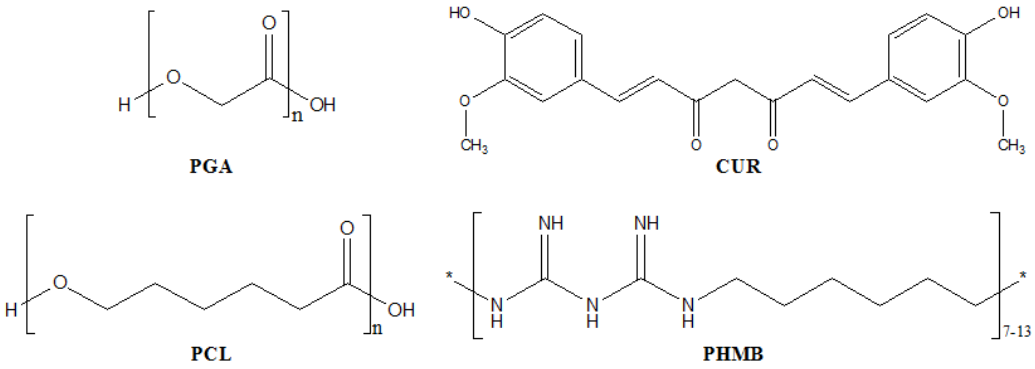

Figure 1

Keridou *et al.*

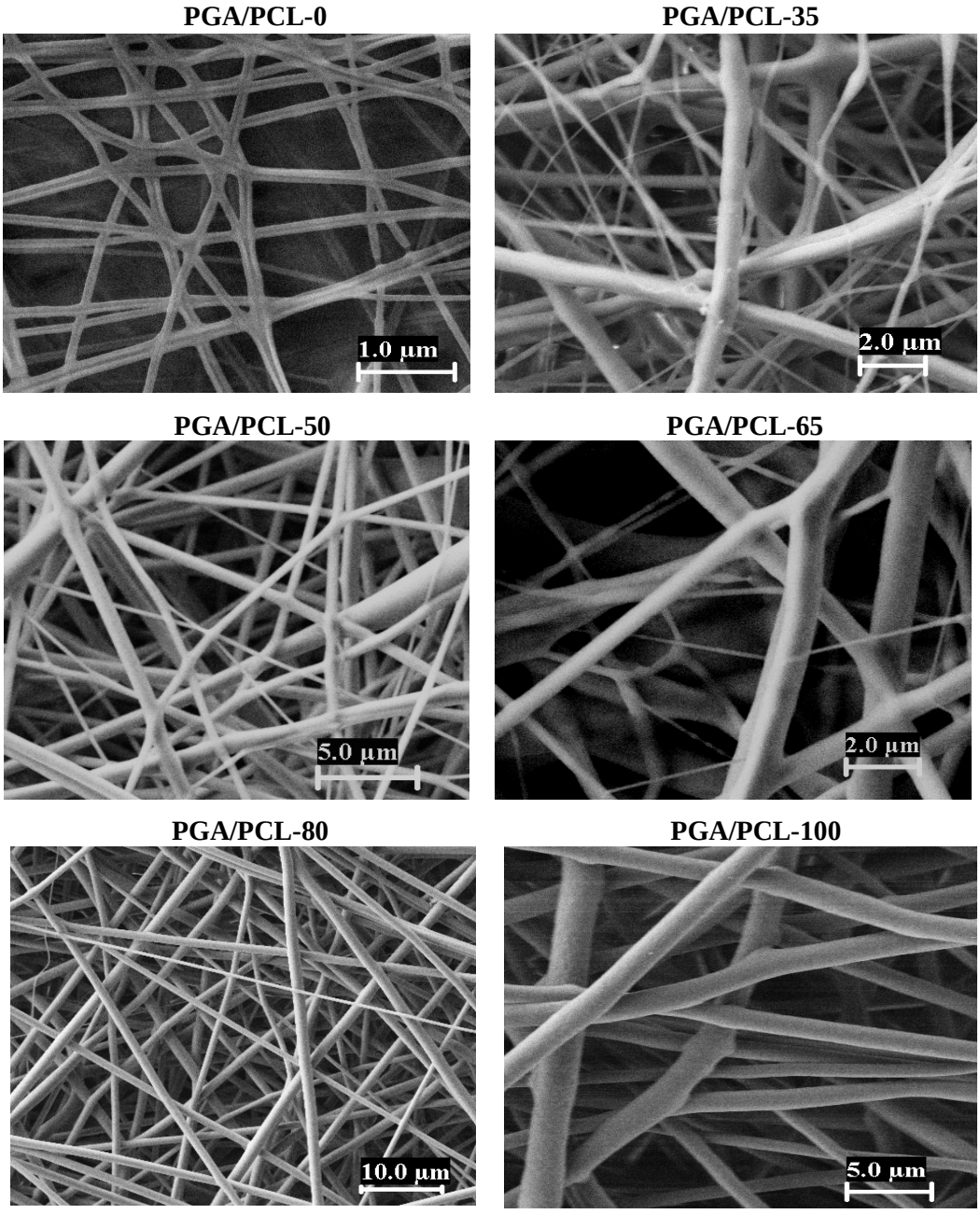

Figure 2

Keridou *et al.*

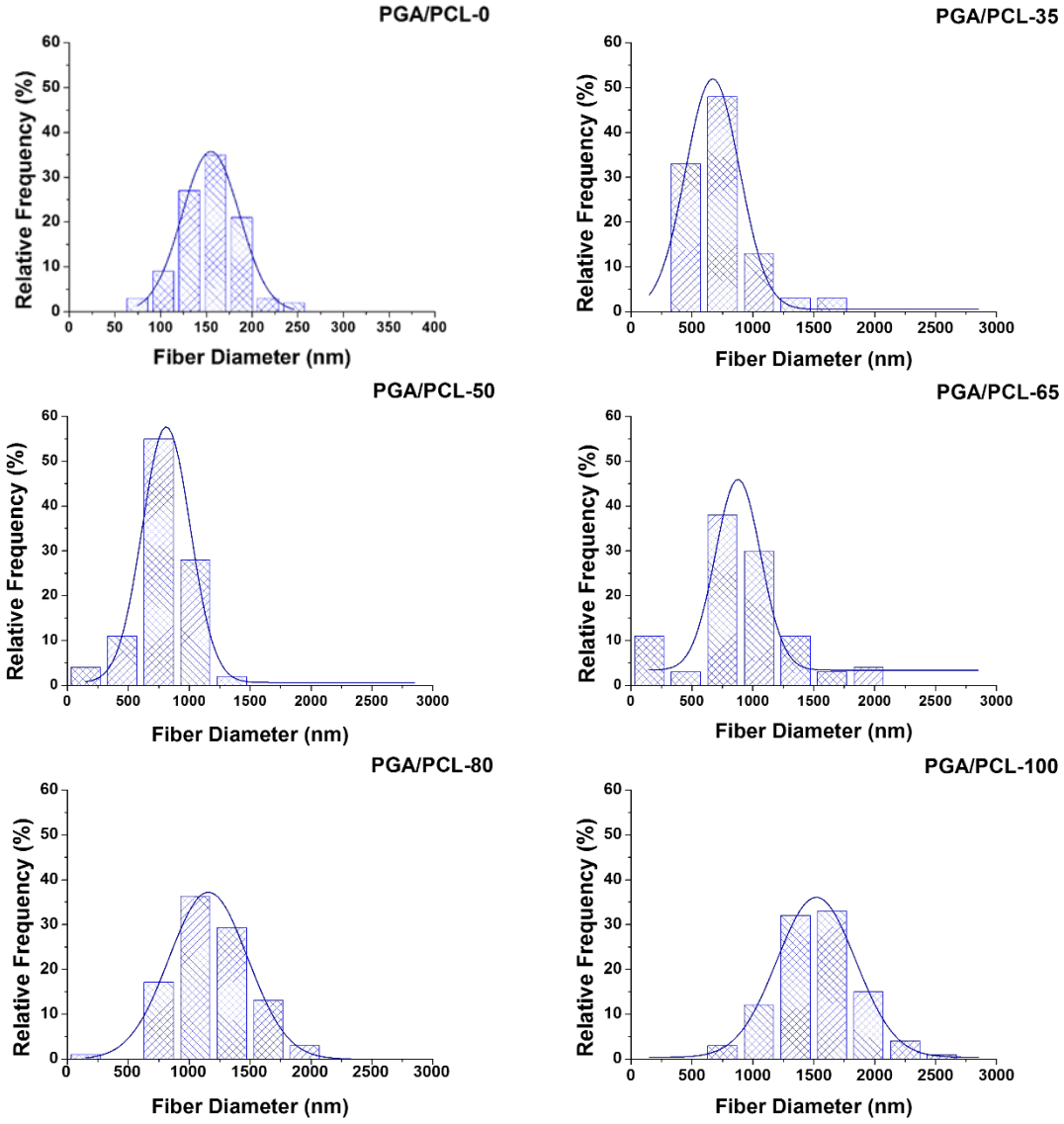

Figure 3

Keridou *et al.*

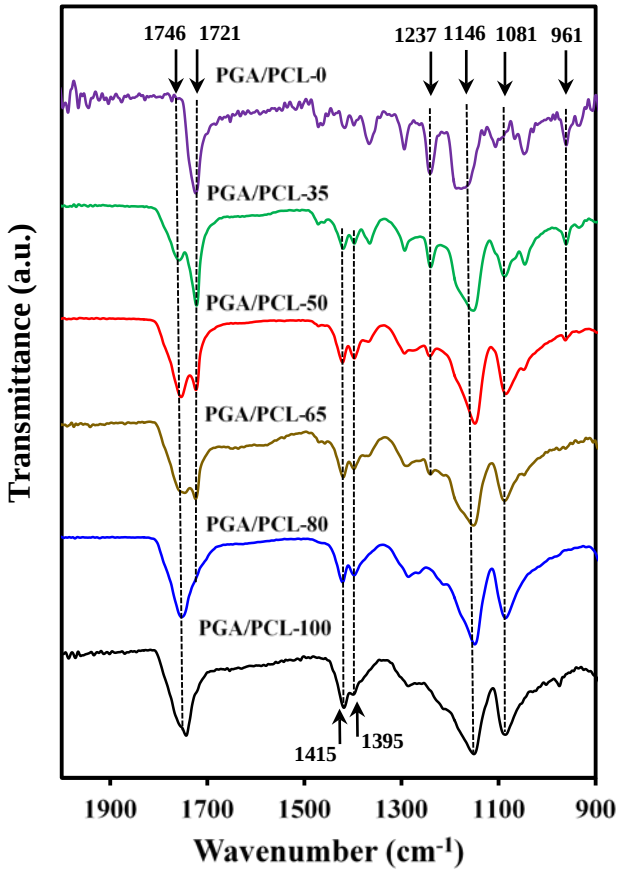

Figure 4

Keridou *et al.*

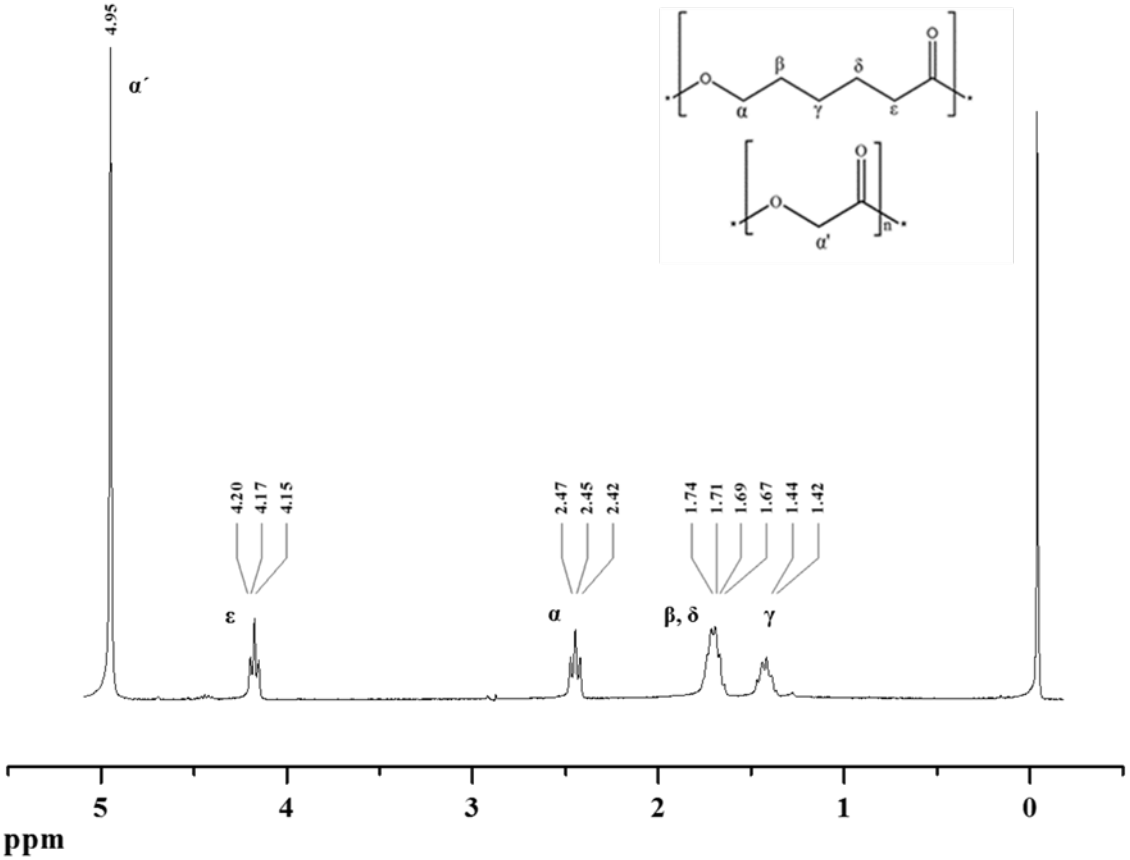

Figure 5

Keridou *et al*.

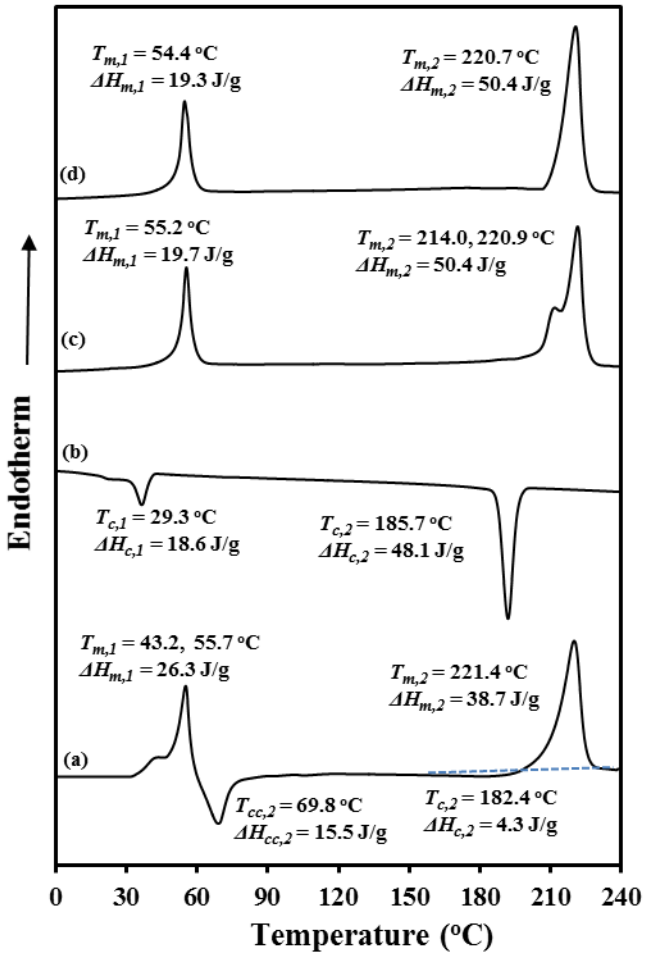

Figure 6

Keridou *et al.*

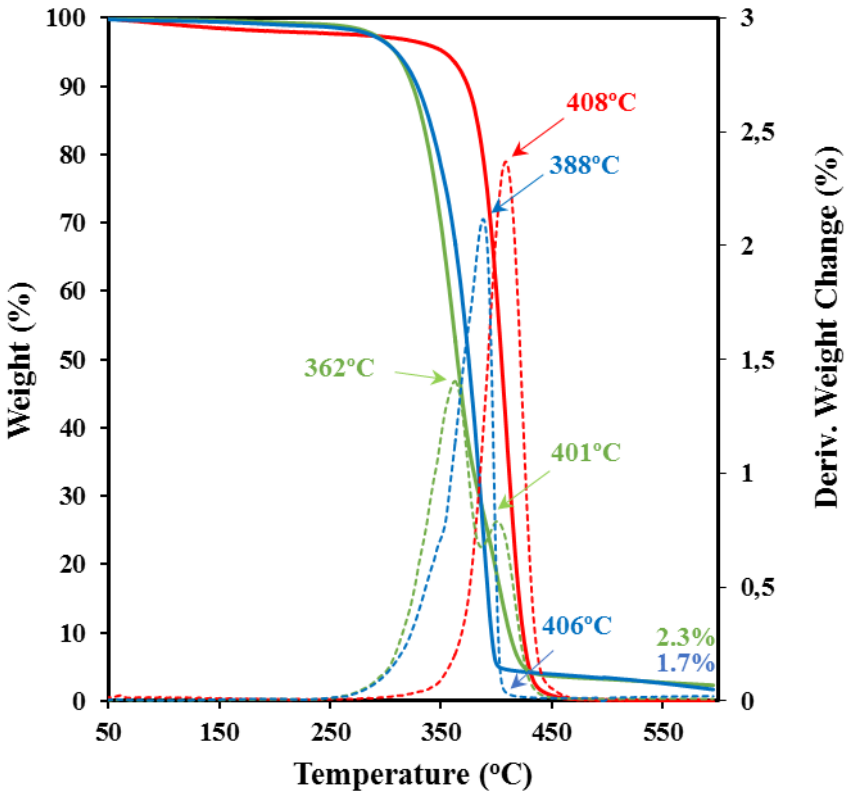

Figure 7

Keridou *et al.*

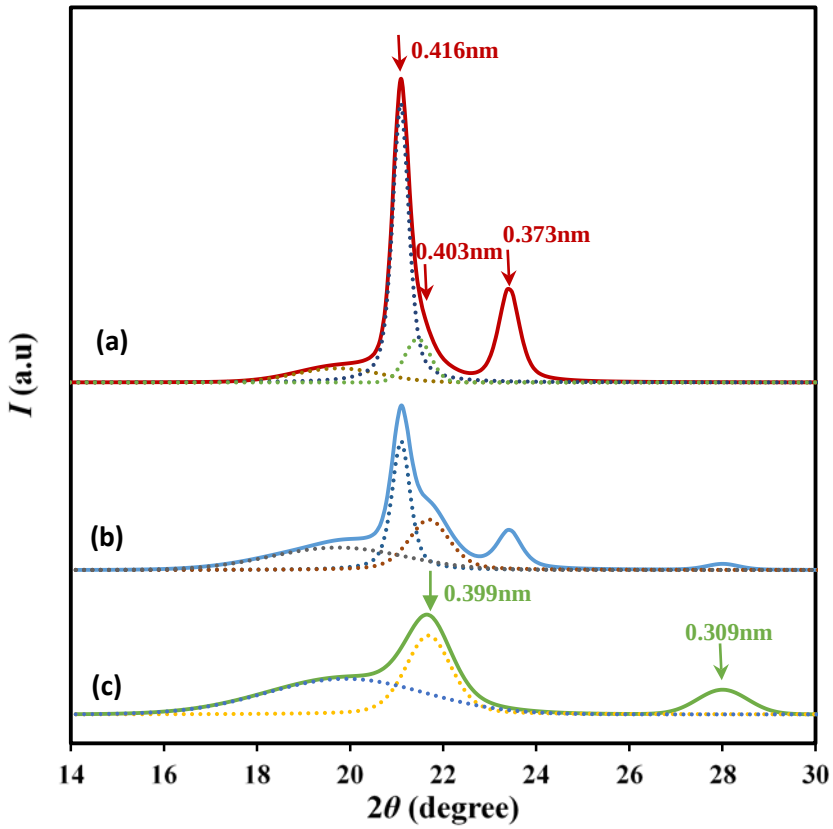

Figure 8

Keridou *et al.*

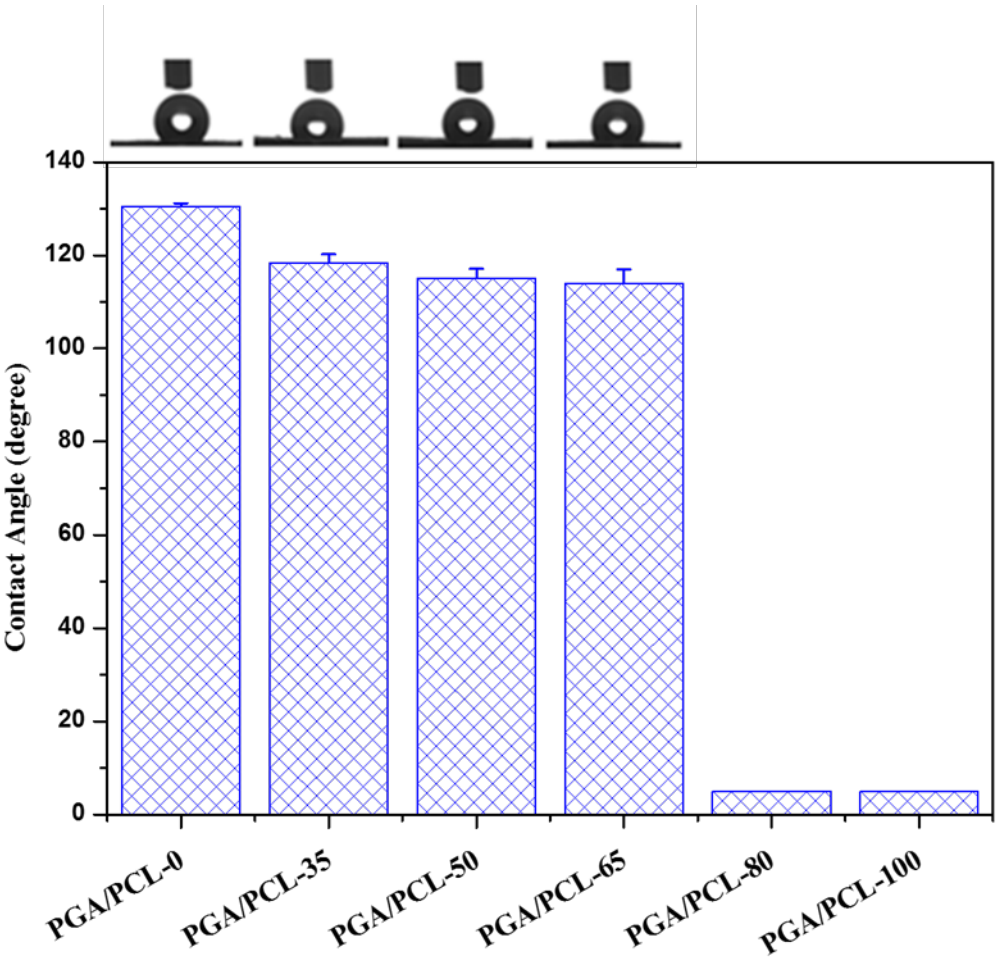

Figure 9

Keridou *et al.*

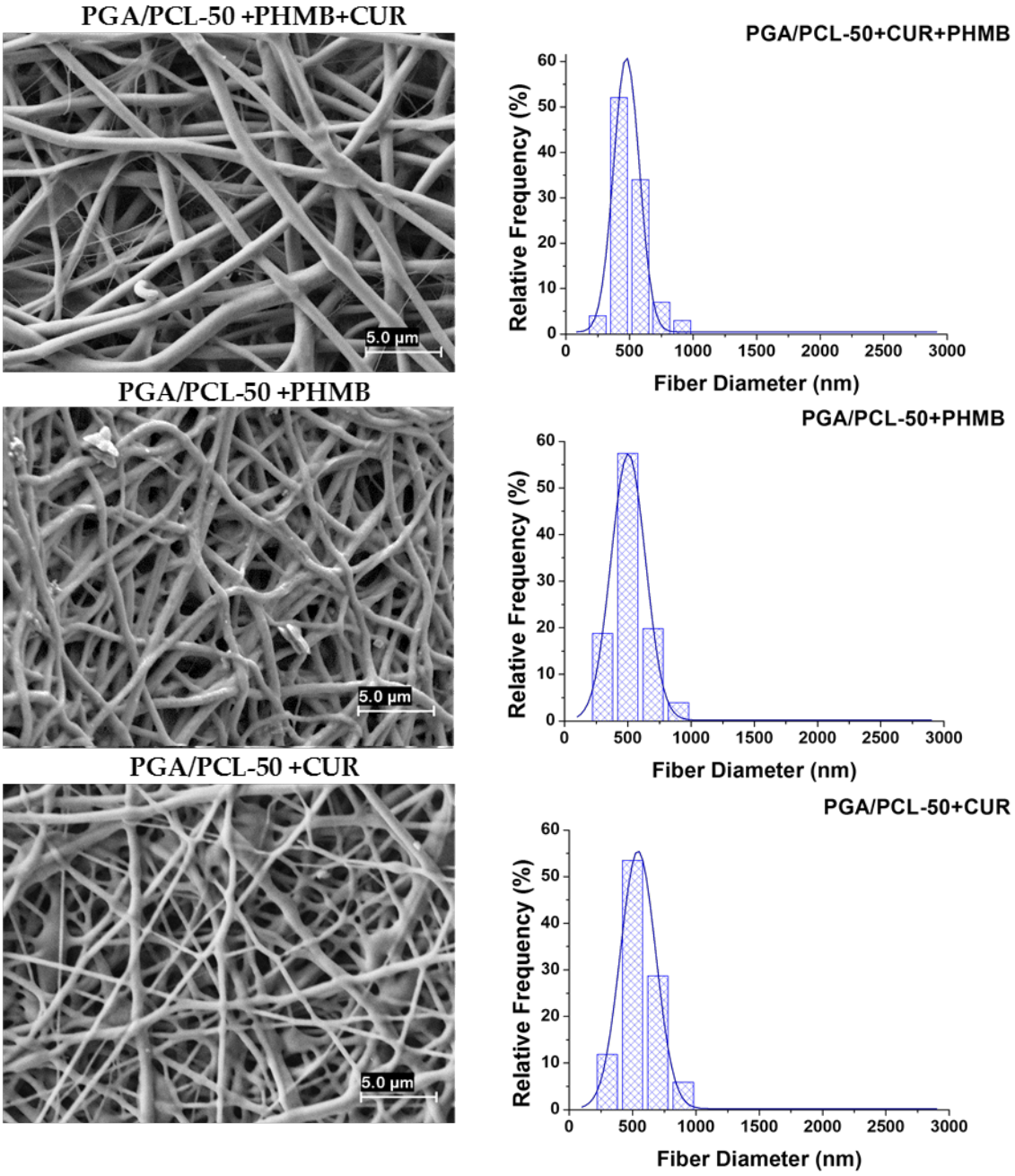

Figure 10

Keridou *et al.*

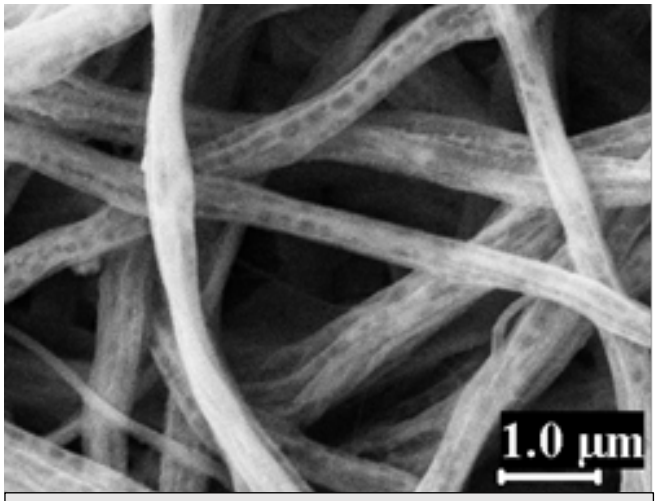

PGA/PCL-50 +PHMB+CUR

Figure 11

Keridou *et al*.

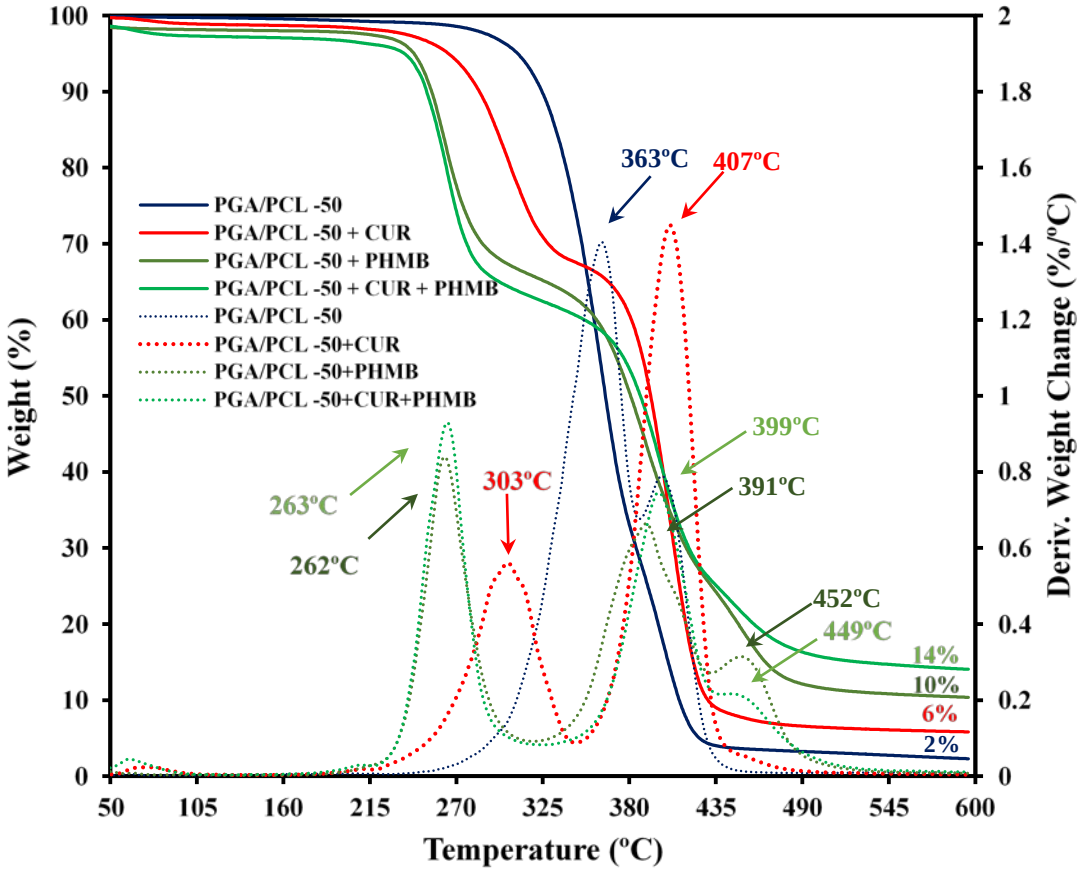

Figure 12

Keridou *et al.*

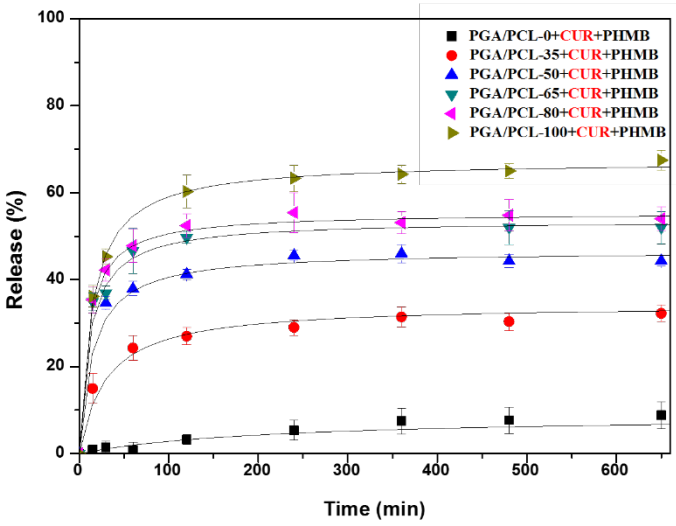

(a)

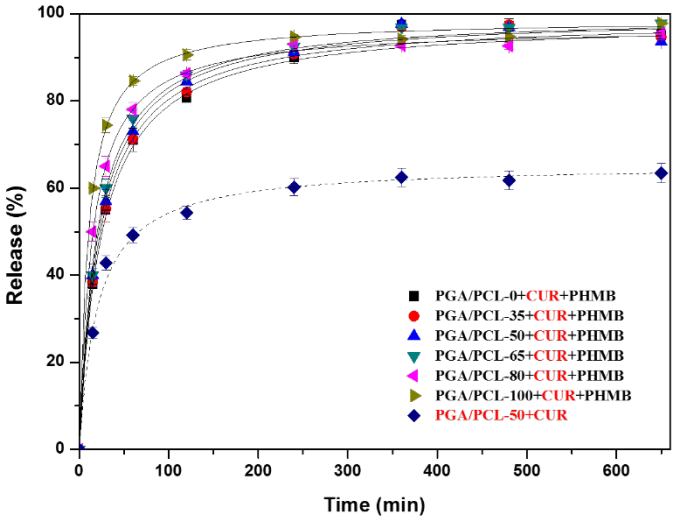

(b)

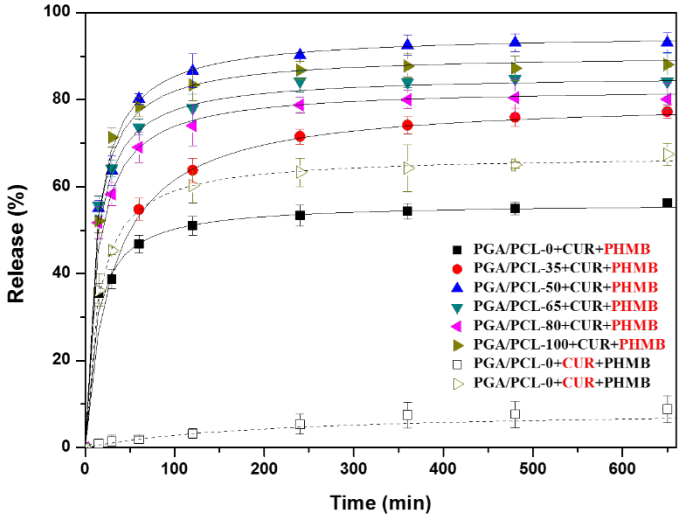

(c)

Figure 13

Keridou *et al.*

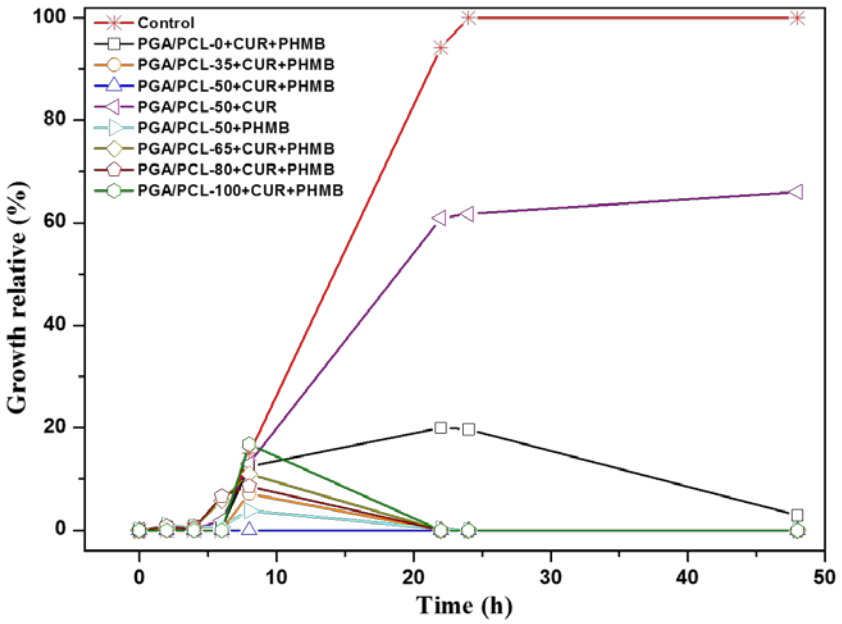

(a)

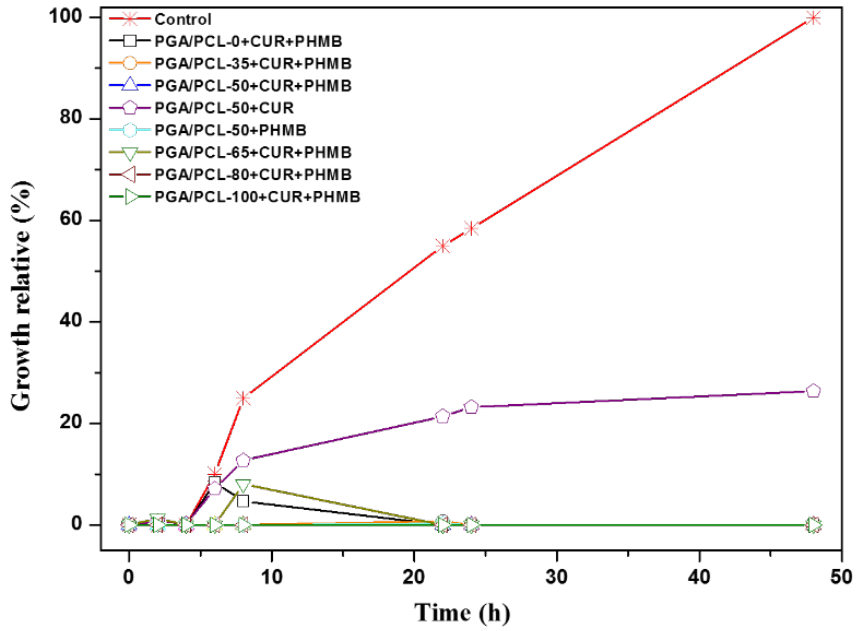

(b)

Figure 14

Keridou *et al.*

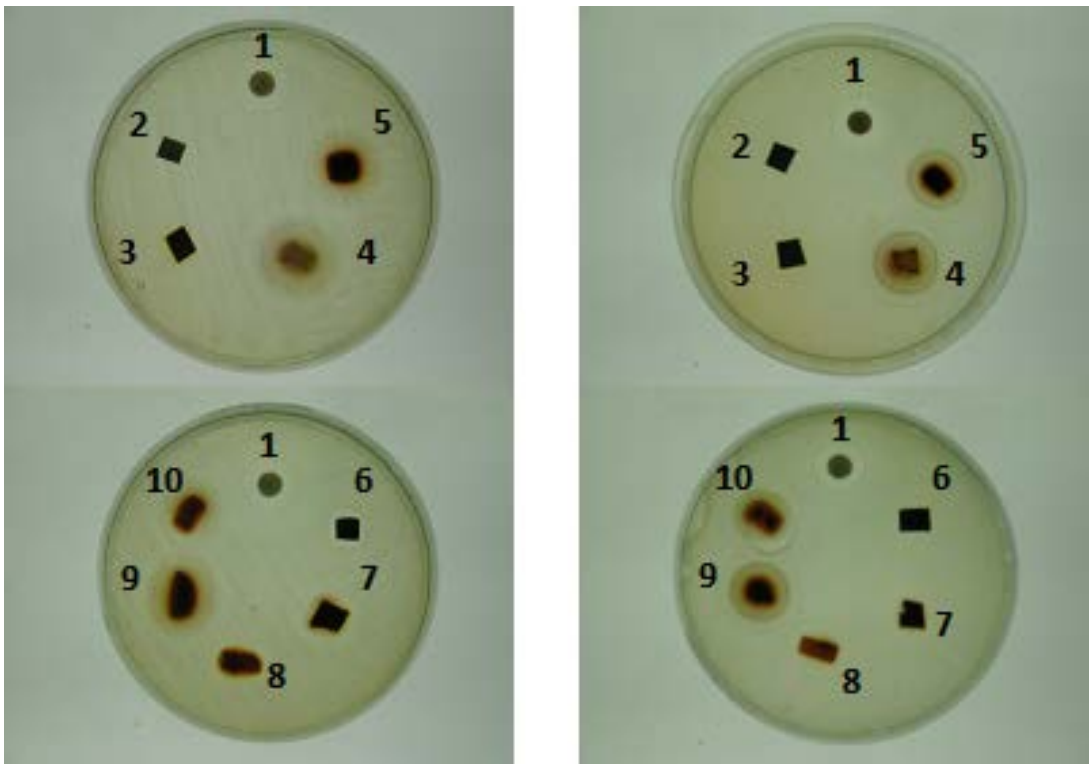

(a) **(b)**

Figure 15

Keridou *et al*.